Algorithm for a Microfluidic Assembly Line

Tobias M. Schneider, Shreyas Mandre, and Michael P. Brenner

School of Engineering and Applied Sciences, Harvard University, 29 Oxford Street, Cambridge, Massachusetts 02138, USA

(Received 27 July 2010; revised manuscript received 27 September 2010; published 28 February 2011)

Microfluidic technology has revolutionized the control of flows at small scales giving rise to new possibilities for assembling complex structures on the microscale. We analyze different possible algorithms for assembling arbitrary structures, and demonstrate that a sequential assembly algorithm can manufacture arbitrary 3D structures from identical constituents. We illustrate the algorithm by showing that a modified Hele-Shaw cell with 7 controlled flow rates can be designed to construct the entire English alphabet from particles that irreversibly stick to each other.

DOI: 10.1103/PhysRevLett.106.094503 PACS numbers: 47.61.Fg, 47.15.gp, 47.85.Np, 81.16.Dn

Developing novel methods for assembling complex structures from small particles has been the focus of much recent investigation [1,2]. Traditional approaches have mostly revolved around designing selective interactions between constituent elements of the assembly. The structure is then assembled in the absence of any external control if thermal fluctuations can drive the system to its energetic ground state [1,3], although nontrivial energy landscapes often render this approach challenging.

Here we consider a different possibility for assembly on small scales, in which microfluidic flow control is used to steer and assemble small particles into structures of high complexity. The basic idea follows from the observation that if we could construct an *arbitrary* time dependent flow field $\vec{v}(\vec{x}, t)$, then particles in the flow could be advected along arbitrary paths and moved to arbitrary locations at a fixed time. This apparently allows us to construct any complex structure, with the individual components binding irreversibly upon contact.

Of course, the flow field $\vec{v}(\vec{x}, t)$ cannot be arbitrary; it must conserve mass and momentum [4],

$$\boldsymbol{\nabla} \cdot \vec{v} = 0, \qquad -\nabla p + \mu \nabla^2 \vec{v} + \rho \vec{b} = 0, \tag{1}$$

where p is the pressure, μ the liquid viscosity, and $\vec{b}$ a volumetric force. The question of what structures can be built thus hinges on what flow fields can be produced using current technology [5], and what are the limits for the possible structures that can form with such flow fields. Volumetric forces can be produced using, e.g., magnetic fields [6] or optical tweezers [7]; alternatively, the flow can be generated by inlets specifying $\vec{v}$ at the boundary of a cell.

We analyze the case where pressure inlets around the boundary force the flow (Fig. 1) and $\vec{b} = 0$. Fluid mechanical constraints prohibit simultaneous control of many particles with this device; however, we demonstrate that a sequential assembly algorithm allows the assembly of arbitrary structures. The device can be designed to manufacture the entire English alphabet using 7 controlled flow rates in two dimensions.

Linear response to boundary forcing.—Consider N particles suspended in the flow domain Ω with their instantaneous positions being $\vec{x}_j$, $j = 1, 2, \ldots, N$. Let the flow be forced on the boundary of the flow cell by a prescribed velocity $\vec{v}(\vec{x}, t)$, $\vec{x} \in \partial\Omega$. The linearity of (1) implies the velocity of the suspended particles is linear in the boundary forcing [4], i.e.,

$$\sum_{k=1}^{N} R_{jk} \dot{\vec{x}}_k = \int_{\partial\Omega} K_j(\vec{x}_1, \vec{x}_2, \ldots, \vec{x}_N; \vec{\xi}) \vec{v}(\vec{\xi}, t) dS + \vec{F}_j, \tag{2}$$

where $\vec{F}_j$ is the force acting on the jth particle, possibly due to nonhydrodynamic interparticle interactions. The response coefficients K_j and R_{jk} depend on the geometry of the flow cell [8] and can be computed numerically. If the boundary forcing occurs through M discrete inlets of area ΔS, located at $\vec{\xi}_k$ with prescribed velocities $\vec{v}_k$, $k = 1, 2, \ldots, M$, then Eq. (2) can be written as

$$\underline{\underline{R}}(\underline{x}) \dot{\underline{x}} = \underline{\underline{M}}(\underline{x}) \cdot \underline{f} + \underline{F}, \tag{3}$$

with $\underline{x} = [\vec{x}_1, \vec{x}_2, \ldots, \vec{x}_N]$, flow rates $\underline{f} = [\vec{v}_1, \vec{v}_2, \ldots, \vec{v}_M]\Delta S$, and $\underline{\underline{M}}_{jk} = K_j(\vec{x}_1, \vec{x}_2, \ldots, \vec{x}_N; \vec{\xi}_k)$.

Equation (3) is an instantaneous linear relation between the imposed flow rates and the particle velocities. This implies that *prescribed* particle trajectories $\underline{x}(t)$ may be realized by imposing suitable $\underline{f}$ obtained by inverting (3). The feasibility of this method then hinges crucially upon invertibility of $\underline{\underline{M}}$, which in general need not be square.

Condition for controlling particle trajectories.—A necessary condition for inverting $\underline{\underline{M}}$ is that the number of independent controls exceed the number of degrees of freedom. With N particles in 3 dimensions, there must be at least $M = 3N + 1$ flow inlets; $3N$ inlets control particle degrees of freedom, with the additional inlet enforcing volume conservation. Similarly, in two dimensions at least $2N + 1$ flow inlets are required.

In general, these algebraic conditions are not sufficient for the practicality of this assembly method. We will see below that, in practice, the flow rates required to independently steer large number of particles can be too

large to be practical, owing to the poor conditioning of the matrix $\underline{\underline{M}}$.

Hele-Shaw flow as a specific example.—To explore this in more detail, we consider a specific example. We consider the fluid mechanics of typical microfluidic devices [9] where the vertical gap thickness H is much smaller than the lateral extent. In Hele-Shaw approximation [8], the velocity profile across the gap is a parabola, with the gap-averaged velocity $\vec{u}$ being proportional to the gradient of the pressure field p satisfying Laplace's equation. A particle at position $\vec{x}_k$ responds to the flow by moving at a speed proportional to the local fluid velocity, $\dot{\vec{x}}_k = \beta\vec{u}(\vec{x}_k)$, with β depending on the particle size and shape [8]. This linear dependence of the particle velocity on the gap-averaged fluid velocity is a general consequence of the linearity of Stokes flow. The quantitative value for β can be calculated in two different limits: If the particle is much smaller than the gap, it is advected by the local velocity, so β depends on the location of the particle relative to the walls. Alternatively, if the particle approximately spans the gap width, the separation of scale underlying the Hele-Shaw approximation breaks down near the particle. The factor β can now be calculated by solving the Stokes equations close to the particle, matching the solution with the parabolic Hele-Shaw flow in the far field.

We consider the device depicted in Fig. 1(a), a circular domain of radius a with flow rates f_k prescribed at the boundary at M discrete inlets with positions $\vec{R}_k$. The velocity field at any position $\vec{x}$ is then given by

$$\vec{u}(\vec{x}) = -\frac{1}{\pi H}\sum_{k=1}^{M}\frac{\vec{x}-\vec{R}_k}{(\vec{x}-\vec{R}_k)^2}f_k \equiv \underline{\underline{B}}(\vec{x})\cdot\underline{f}. \qquad (4)$$

Thus, the matrix $\underline{\underline{M}}$ in Eq. (3) may be constructed by combining the N position dependent matrices $\underline{\underline{B}}(\vec{x}_i)$ corresponding to each particle.

We first test whether this flow cell will allow simultaneous control of all N particles by boundary inlets. The flow rates scale inversely with the duration of the assembly so that the scale for the flux depends on the chosen time scale. We scale flow rate by the flux required to move a single particle across the cell $F = \pi a H\delta/\tau$, where δ is the width of the inlet and the duration τ of the process. Figure 1(b) shows that if we require the particles to be transported in straight lines at constant velocity from their initial position to their final position, the required flow rates reach up to 30 times this value. This happens because when two or more particles are moving towards each other a distance ϵ apart, a strain rate of $\dot{\epsilon}/\epsilon$ is required. If the approach velocity is constant, the strain diverges as $\epsilon \to 0$, implying diverging flow rates. Thus, whenever particles are brought together at constant velocity, large fluxes are required.

Optimized trajectories.—We can try to reduce the flow rates by choosing the particle trajectories and speeds connecting the initial and the final states to minimize this effect. Intuitively, we can decrease the speed of the particles as they approach each other to minimize the required flow rates. To find out if this is sufficient we compute the optimal trajectories connecting the initial to the desired particle configuration by finding the trajectories that minimize dissipation. The dissipation rate is given by

$$w = \frac{H^2}{12\mu}\int_A |\nabla p|^2 dA. \qquad (5)$$

For the discretized forcing w can be expressed as a quadratic form in the flow rates $w = \underline{f}^\dagger\cdot\underline{\underline{D}}\cdot\underline{f}$ with metric $\underline{\underline{D}}$ being analytically given in terms of the inlet positions. We minimize the dissipation and thereby the flow rates under the constraints that the dynamics move the particles according to their equation of motion Eq. (3) from their chosen initial state to their final state. This requires that we find the trajectories that minimize the Lagrangian

$$\mathcal{L} = \int_0^1 dt\{\underline{f}^\dagger\cdot\underline{\underline{D}}\cdot\underline{f} - \underline{\lambda}^\dagger\cdot[\underline{\dot{x}} - \underline{\underline{M}}\cdot\underline{f}] - \gamma\underline{e}^\dagger\cdot\underline{f}\}, \qquad (6)$$

where $\underline{\lambda}$ and γ are Lagrange multipliers to enforce the constraints and $\underline{e}^\dagger = (1,\ldots,1)$. λ enforces the equation of

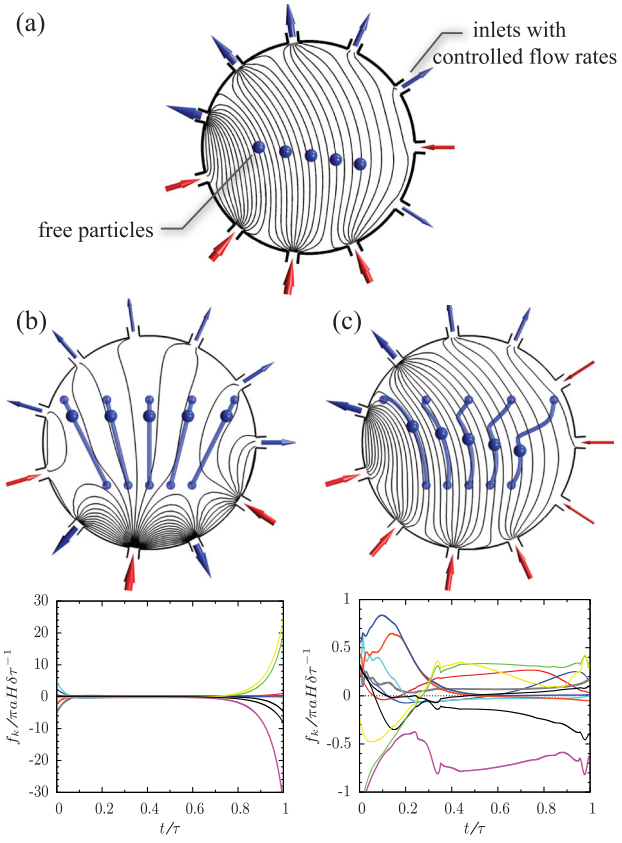

FIG. 1 (color online). (a) Schematic: Five particles are advected by the flow field in a circular cell. The flow field, visualized by its streamlines, is set up by 11 flow rates imposed on the boundary (arrows indicating the strength and direction). (b),(c) Two trajectories transporting particles from a fixed initial position to their desired final position with the required flow rates. The linear trajectory (b) requires flow rates almost 2 orders of magnitude higher than the trajectory in (c). This optimized trajectory minimizes dissipation.

motion, whereas γ requires that the fluxes $\underline{f}$ satisfy volume conservation.

To minimize $\mathcal{L}$ we consider a small perturbation of the flow rates in the direction of steepest descent, i.e., $\underline{f} \to \underline{f} + \underline{\Delta f}$ with

$$\underline{\Delta f} = -\epsilon \left(\frac{\delta \mathcal{L}}{\delta \underline{f}}\right)^{\dagger} = -\epsilon \{2\underline{\underline{D}} \cdot \underline{f} + \underline{\underline{M}}^{\dagger} \cdot \underline{\lambda} - \gamma \underline{e}\}. \quad (7)$$

To fix the unknown fields γ and $\underline{\lambda}$, we require the variation of $\mathcal{L}$ with respect to $\underline{x}$, $\underline{\lambda}$, and γ to vanish for the updated flow rates and trajectory $\underline{x} \to \underline{x} + \underline{\Delta x}$. Evaluating the stationarity condition at linear order in the increments allows us to eliminate γ from Eq. (7) and selects a unique solution of the *adjoint* equations

$$\dot{\lambda}_k = -f_n \frac{\partial M_{mn}}{\partial x_k} \lambda_m \quad (8)$$

which are numerically solved together with the evolution of $\underline{x}$ using MATLAB [10].

The minimization starts from the linear trajectory in Fig. 1(b) along which we choose velocity variations damping large peak flow rates. Figure 1(c) shows the same 5 particles following an optimized trajectory for which the flow rates are reduced by more than an order of magnitude to the desired range. The reduction is due to choosing $\dot{\epsilon}/\epsilon$ to approach a finite number as $\epsilon \to 0$. Thus, optimizing trajectories can lead to simultaneous control of a modest number of particles using boundary flow rates.

Nonetheless, this approach does not scale to larger number of particles; e.g., we could not find trajectories allowing simultaneous control of 13 particles required to spell the letter "*B*" at moderate fluxes. This reflects an implementation independent physical limit of directing flow fields with boundary fluxes, resulting from the fact that flow modes forced at the boundary decay in amplitude as one moves away from the wall. The characteristic length scale governing the decay of the boundary modes is the distance between the injection points which scales inversely with the number of inlets. But as the particle number increases, we need more inlets to control the particle motion. This limits the number of particles that can be controlled simultaneously. We could not find trajectories transporting more than 6 individual particles at moderate flow rates.

Sequential assembly.—To overcome this physical limitation, an algorithm is required that decouples the number of controlled degrees of freedom from the number of particles in the desired structure. This can be achieved with a sequential approach, where one particle after the other is attached to an aggregate which moves as a rigid body subject to force and torque balance. Construction of the corresponding $\underline{\underline{M}}$ matrix requires explicitly accounting for the translation and rotation of the cluster consisting of Z particles at positions $\vec{x}_\alpha = \vec{x}_{cm} + \underline{\underline{R}}(\varphi)(\vec{\xi}_\alpha - \vec{\xi}_{cm})$, where $\vec{\xi}_\alpha$ are the prescribed particle positions in the aggregate's frame of reference and $\underline{\underline{R}}$ is the two-dimensional rotation. How many degrees of freedom are required for the assembly? Controlling the position of the aggregate requires 2 degrees of freedom. Rotating it requires a stagnation point flow superimposed on the local mean flow near the aggregate. This requires independent control of 2 more degrees of freedom, the strength and orientation of the stagnation point flow. Finally, the free particle location demands 2 additional degrees of freedom. Including volume conservation we thus need 7 inlets to absolutely control all degrees of freedom.

Sequentially adding particles allows us to assemble structures of arbitrary shape and thus spell a word (Fig. 2) without any feedback control. Technically, the trajectory for a particle to be added is constructed by defining the desired position which is taken from [11] and the direction of approach in the frame of reference of the aggregate. Spline interpolation between the initial position of the new particle and its final position when the aggregate has reached the desired configuration then yields the particle path. The aggregate can also be moved arbitrarily; we choose to keep its orientation fixed and move the center of mass to the device center in each step. The velocity along this trajectory is chosen such that it vanishes at the initial and final configuration so

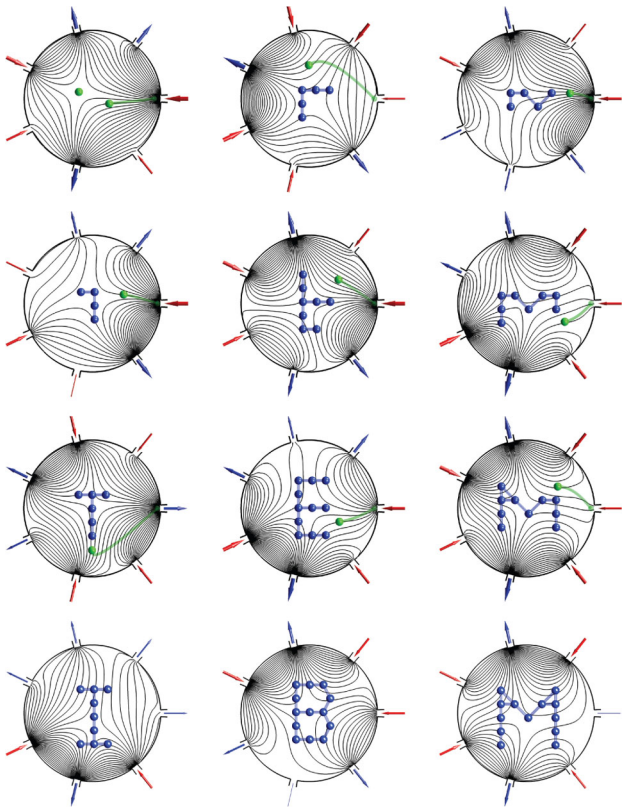

FIG. 2 (color online). Sequentially particles are added to form aggregates of arbitrary shape. The three columns present snapshots along the assembly of three example structures presented in the last row. The required time variations of the 7 controlled flow rates are computed *a priori* (e.g., Fig. 3). See movie M1 in Ref. [14] for an animation.

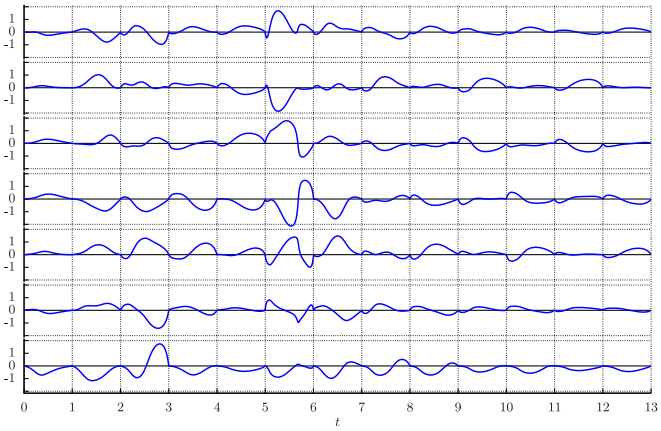

FIG. 3 (color online). Flow rates $f_k/\pi a H \delta \tau^{-1}$ for the 7 inlets as a function of time t/τ. These allow us to spell the letter "B." At each integer time a new particles enters the cell.

that flow rates reach zero after each assembly step. With this choice of trajectories, the flow rates are computed inverting Eq. (3). No extensive optimization was required to limit the fluxes (see Fig. 3) to reasonable values of the same order as those in Fig. 1(c). Optimizing trajectories might, however, still be useful either to further reduce the required flow rates or to minimize internal forces within the growing aggregate so that the forming structure can sustain the stresses in the flow.

We envision a typical mode of operation of the microfluidic device similar to that of a macroscopic robotic assembly line: Once the constituents of an assembly and the detailed assembly sequence are decided on, the flow rates on the inlets of the device and the precise instants at which each constituent is introduced are calculated. These precomputed flow rates are then set up in a time-periodic fashion, and a train of the assembly constituents is introduced at the inlets of the device to accomplish a train of assembled products.

In summary, we have shown that microfluidic assembly can be an efficient strategy if structures are built sequentially. Using this approach, we show that the temporal control of only 7 flow rates allows us to build arbitrarily shaped particle aggregates in two dimensions. In three dimensions, the same argument implies that 11 different flow rates are required. Different chamber geometries and hydrodynamic interactions can be incorporated into this framework, which rests solely on the linearity of Stokes flow. We anticipate that similar algorithms can be constructed using other forcing mechanisms such as electrokinetics [12], where nonhydrodynamic electrical forcing contributions need to be included into the transfer matrices. A challenge for practical implementation is to quantify the sensitivity of particle trajectories to noise in the imposed flow rates. This is particularly relevant when scaling down the assembly to submicron scale, where the Peclét number corresponding to Brownian motion is small and hence potentially disruptive. One option for dealing with errors and noise is to implement feedback control [13], though this significantly complicates the process. Another intriguing possibility is to simply embrace the existence of stochasticity and construct the most stable trajectories that maximize the probability of formation of the desired structures in the presence of noise. Finding algorithmic methods for carrying out this optimization is an important direction for future research.

We acknowledge support by the NSF, through grants DMS-0907985 and DMR-0820484, the Kavli Institute for Bionano Science and Technology, and the DFG, through grant Schn 1167/1 (T. M. S.).

[1] G. Whitesides and B. Grzybowski, Science **295**, 2418 (2002).
[2] H.-Y. J. Yeh and J. S. Smith, IEEE Photonics Technol. Lett. **6**, 706 (1994); G. Whitesides and M. Boncheva, Proc. Natl. Acad. Sci. U.S.A. **99**, 4769 (2002); R. R. A. Syms *et al.*, J. Microelectromech. Syst. **12**, 387 (2003); C. Dobson, Semin. Cell. Dev. Biol. **15**, 3 (2004); M. Boncheva and G. Whitesides, MRS Bull. **30**, 736 (2005); G. Meng *et al.*, Science **327**, 560 (2010).
[3] M. Boncheva *et al.*, Proc. Natl. Acad. Sci. U.S.A. **102**, 3924 (2005); M. Fialkowski, A. Bitner, and B. Grzybowski, Nature Mater. **4**, 93 (2004); P. W. K. Rothemund, Nature (London) **440**, 297 (2006); S. Douglas *et al.*, Nature (London) **459**, 414 (2009).
[4] J. Happel and H. Brenner, *Low Reynolds Number Hydrodynamics: with Special Applications to Particulate Media* (Kluwer, Dordrecht, 1991).
[5] S. Quake and A. Scherer, Science **290**, 1536 (2000); B. D. Gates *et al.*, Annu. Rev. Mater. Res. **34**, 339 (2004); T. Squires and S. Quake, Rev. Mod. Phys. **77**, 977 (2005); G. Whitesides, Nature (London) **442**, 368 (2006); J.-H. Jang *et al.*, Angew. Chem., Int. Ed. **46**, 9027 (2007); D. Dendukuri and P. S. Doyle, Adv. Mater. **21**, 4071 (2009); D. K. Hwang, D. Dendukuri, and P. S. Doyle, Lab Chip **8**, 1640 (2008); K. Sung *et al.*, J. Am. Chem. Soc. **130**, 1335 (2008).
[6] M. C. Jullien, J. Paret, and P. Tabeling, Phys. Rev. Lett. **82**, 2872 (1999); N. T. Ouellette, P. J. J. O'Malley, and J. P. Gollub, Phys. Rev. Lett. **101**, 174504 (2008).
[7] E. Dufresne and D. Grier, Rev. Sci. Instrum. **69**, 1974 (1998); D. Grier, Nature (London) **424**, 810 (2003).
[8] C. Pozrikidis, J. Fluid Mech. **261**, 199 (1994).
[9] Y. Xia and G. M. Whitesides, Annu. Rev. Mater. Sci. **28**, 153 (1998); M. Hashimoto *et al.*, Soft Matter **4**, 1403 (2008).
[10] Since the trajectory increment preserves constraints to linear order only, we explicitly enforce in each iteration that particles reach their prescribed final positions exactly. This corrects for neglected higher order effects.
[11] D. M. Eigler and E. K. Schweizer, Nature (London) **344**, 524 (1990).
[12] A. E. Cohen, Phys. Rev. Lett. **94**, 118102 (2005).
[13] A. E. Cohen and W. E. Moerner, Proc. Natl. Acad. Sci. U.S.A. **103**, 4362 (2006).
[14] See supplemental material at http://link.aps.org/supplemental/10.1103/PhysRevLett.106.094503 for an animation of the assembly process.